

Probing the Neuraminidase Activity of Influenza Virus Using a Cytolysin A Protein Nanopore

Dong-Kyu Kwak,^{||} Jin-Sik Kim,^{||} Mi-Kyung Lee, Kyoung-Seok Ryu, and Seung-Wook Chi*Cite This: <https://dx.doi.org/10.1021/acs.analchem.0c03399>

Read Online

ACCESS |



Metrics & More

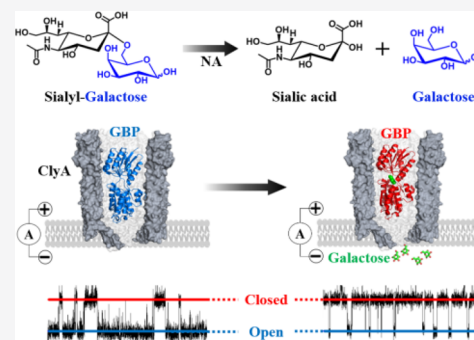


Article Recommendations



Supporting Information

ABSTRACT: Neuraminidase (NA), one of the major surface glycoproteins of influenza A virus (IAV), is an important diagnostic biomarker and antiviral therapeutic target. Cytolysin A (ClyA) is a nanopore sensor with an internal constriction of 3.3 nm, enabling the detection of protein conformations at the single-molecule level. In this study, a nanopore-based approach is developed for analysis of the enzymatic activity of NA, which facilitates rapid and highly sensitive diagnosis of IAV. Current blockade analysis of the D-glucose/D-galactose-binding protein (GBP) trapped within a type I ClyA-AS (ClyA mutant) nanopore reveals that galactose cleaved from sialyl-galactose by NA of the influenza virus can be detected in real time and at the single-molecule level. Our results show that this nanopore sensor can quantitatively measure the activity of NA with 40–80-fold higher sensitivity than those previously reported. Furthermore, the inhibition of NA is monitored using small-molecule antiviral drugs, such as zanamivir. Taken together, our results reveal that the ClyA protein nanopore can be a valuable platform for the rapid and sensitive point-of-care diagnosis of influenza and for drug screening against the NA target.



Influenza A viruses (IAV) cause an acute respiratory disease and severe pandemics with a high mortality of 250,000–640,000 deaths worldwide each year.¹ IAV can infect a variety of hosts, ranging from waterfowls to mammals.^{2–4} Neuraminidase (NA), one of the major surface proteins of IAV, is known to be involved in important processes of the viral life cycle, such as host infection, viral replication, and high pathogenicity.^{5,6} Hence, NA is a well-known diagnostic biomarker for IAV infection and an important target for therapeutic neutralizing antibodies and small molecule inhibitors.⁷ Briefly, NA is a glycoside hydrolase that cleaves the terminal sialic acids from substrates, including glycoproteins, glycolipids, and oligosaccharides.⁸ In particular, IAV NA has been shown to cleave the terminal sialic acid residues from the glycan of host cell receptors.⁹ This enzymatic activity of NA is known to play essential roles in the spreading of the influenza virus because it has been demonstrated to be responsible for the release of newly formed viruses from the infected host cell to new target cells, the prevention of the virus aggregation, and the suppression of the rebinding via hemagglutinin to the host cell.^{10,11}

Currently, there are two types of conventional methods used for the diagnosis of IAV infection.^{12,13} The first is employment of molecular assays, including viral culture and reverse transcriptase polymerase chain reaction (RT-PCR), whereas the other is the use of antigen detection tests, including rapid influenza diagnostic test (RIDT) and immunofluorescence assays. However, because of the time-consuming, labor-intensive process (for viral culture and RT-PCR) and low

sensitivity of detection (for RIDT and immunofluorescence assays), there is a high demand for novel technologies for the point-of-care diagnosis of influenza.^{14,15} In particular, it is necessary to overcome the limitation of the sensitivity for the point-of-care diagnosis of influenza at an early stage of the viral infection.

Nanopore is an emerging, high precision biosensor, allowing the detection of subtle conformational changes of biomolecules at the single-molecule level.¹⁶ When electrical potential is applied to the nanometer-sized pore, the ionic flux across the nanopore generates an electrical nanopore signal. Analytes passing through the nanopore induce the interference of the ionic current, which is characterized by dwell time and current blockade. Nanopore biosensors have been used for genome sequencing,¹⁷ detection of diverse individual biomolecules,^{18–21} biomolecular interactions, conformational changes, and enzymatic reactions.^{22–24} Cytolysin A (ClyA) is a pore-forming protein, known to form dodecameric to tetradecameric nanopores with an internal constriction of over 3.3 nm.²⁵ In previous reports, a ClyA nanopore was studied to monitor the conformational changes of diverse biomolecules, protein–

Received: August 11, 2020

Accepted: October 6, 2020

ligand interactions, enzymatic reactions, and quantitative analysis.^{16,26,27} This engineered ClyA nanopore (ClyA-AS) with mutations in key residues revealed remarkable improvements in nanopore properties and stability in planar lipid bilayers.²⁵

In this study, we monitored the enzymatic activity of IAV NA in releasing galactose following cleavage of sialic acid derivatives (SG) through the use of the ClyA-AS nanopore. The ClyA-AS nanopore trapping the D-glucose/D-galactose-binding protein (GBP) allows the detection of trace amounts of the influenza virus NA by sensing the galactose cleaved from SG. Using this nanopore, we performed real-time and single-molecule detection of galactose produced by the NA enzymatic reaction and quantitative measurement of the viral NA activity and probed the inhibitory effects of small-molecule antiviral drugs on the activity of NA.

Prior to measuring galactose at the single-molecule level, we characterized GBP using the *Escherichia coli* type I ClyA-AS nanopore (ClyA hereafter).²⁸ GBP is known to bind specifically to galactose ($K_d = 480$ nM).²⁹ The GBP structure has been found to have open (ligand-free) and closed (ligand-bound) conformations via glucose binding, although NMR studies have reported that the ligand-free state exists in both conformations (Figure 1a).^{30,31} In previous reports, the

closure or gating of the ClyA nanopore. Thus, we applied a voltage of -90 mV throughout this study (Figure 1b). In the absence of galactose, the nanopore events detected for GBP revealed two current levels (L1 = -95 ± 0.25 pA and L2 = -97 ± 0.27 pA), indicating that the trapped GBP inside the nanopore assumes two conformations. Through three independent nanopore experiments ($N = 3$) for free GBP, we observed that the percentage ratios observed between the open pore current and current blockade ($I_{res\%}$) of L1 and L2 were $69.1 \pm 0.8\%$, and $67.4 \pm 0.7\%$, respectively (Figure 1c). The relative event durations of the free GBP at each current level were 28% (L1) and 72% (L2), consistent with the percentage of open (32%) and closed (68%) conformations detected by NMR spectroscopy.³¹

Titration of galactose into the *trans* compartment of the ClyA nanopore (up to $50 \mu\text{M}$) resulted in changes in the relative event durations of L1, corresponding to the closed conformation, from 28% to 83% (Figure 1c). Accordingly, we noted that as the concentration of galactose increased, the number of L1 events was dramatically increased until saturation was achieved at the galactose concentration of $50 \mu\text{M}$. The two current blockades of L1 and L2 reflect two residence sites for GBP protein within the ClyA pore lumen. L1 is associated with GBP residing at a deep, more sterically constrained site, while L2 is related to the protein residing at a position closer to the wider *cis* entrance of the ClyA pore.^{32,33}

The binding of galactose to GBP causes a substantial structural change from open to closed conformation, resulting in a hinge angle change between N- and C-terminal domains (from 134° to 100° , respectively; Figure 1a).³⁰ The more compact GBP–galactose complex structure may be located closer to the narrower *trans* exit of a ClyA pore, resulting in higher current blockades (L1) than those of free GBP protein (L2). Therefore, event duration of the L1 level current increases after galactose binding to GBP.

The fractional time of L1 level events (f_{L1}), corresponding to the normalized fraction of the closed conformation of the galactose–GBP complex, versus the galactose concentration was fitted to a Hill function (Figure 1d). The extrapolated apparent binding constant (K_d^{app}) between GBP and galactose in the GBP-trapped ClyA nanopore was shown to be $0.23 \pm 0.02 \mu\text{M}$, which was similar to those measured in bulk using autofluorescence titration and radiolabeled galactose titration.^{29,34} In addition, we estimated the limit of detection of galactose (LOD^{GAL}) using the GBP-trapped ClyA nanopore. The LOD^{GAL} in the three independent experiments was determined to be 38 nM ($N = 3$).³⁵ This finding indicated that this nanopore sensor has more than 34-fold higher sensitivity over those of existing commercial kits for the detection of galactose ($1.3\text{--}10.0 \mu\text{M}$ in LOD). Taken together, these results showed that galactose could be detected at the single-molecule level using the GBP-trapped ClyA nanopore.

During the process of viral infection, the NA enzyme of IAV has been reported to specifically cleave sialic acid from the surface of host cells to release viral progeny.⁹ To detect the enzymatic activity of NA using the ClyA nanopore, we introduced a sialyl-galactose (SG) substrate that would allow the release of galactose following enzymatic cleavage by NA (Figure 2a).³⁶ We applied the SG substrate and NA from H5N1 (A/Anhui/1/2005) to the *trans* compartment of the GBP-trapped ClyA nanopore (Figure 2b). As previously described,¹⁶ small molecules such as galactose ($0.17 \text{ nm} \times 0.45 \text{ nm} \times 0.62 \text{ nm}$) can freely diffuse through the narrow

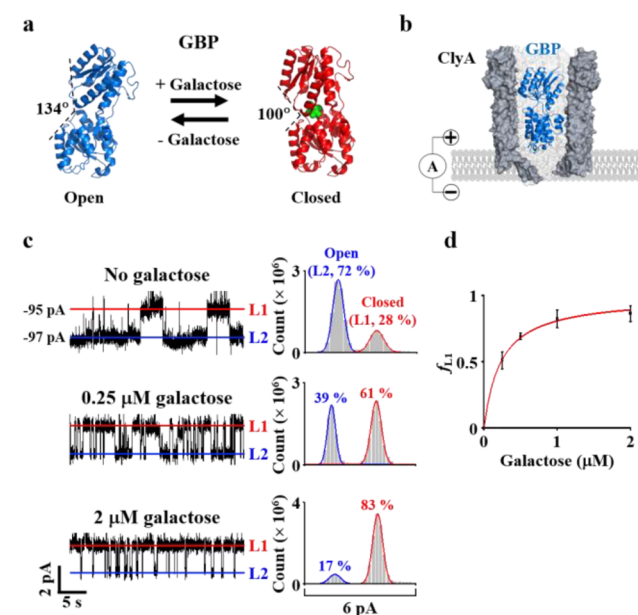


Figure 1. Analysis of galactose binding using the GBP-trapped ClyA nanopore. (a) Illustration of GBP in the ligand-free (open) and ligand-bound (closed) states. (b) Surface depiction of the GBP-trapped ClyA nanopore. (c) Electric current traces in the presence of increasing concentrations of galactose (left). Histograms of event durations of closed (L1) and open (L2) conformations in 30 s of current traces (right). (d) Fractional times of L1 (f_{L1}) versus concentrations of galactose fitted to a Hill function with the coefficient set to 1. Error bars represent standard deviations ($N = 3$).

concentration of glucose was directly measured from biological samples, such as blood, sweat, urine, and saliva, using the ClyA nanopore.¹⁶ To test whether the binding of galactose by GBP could be measured using the ClyA nanopore, 50 nM GBP was added to the *cis* compartment of the ClyA nanopore. Applying voltages lower than -90 mV caused release of trapped GBP, while applying voltages higher than -90 mV induced self-

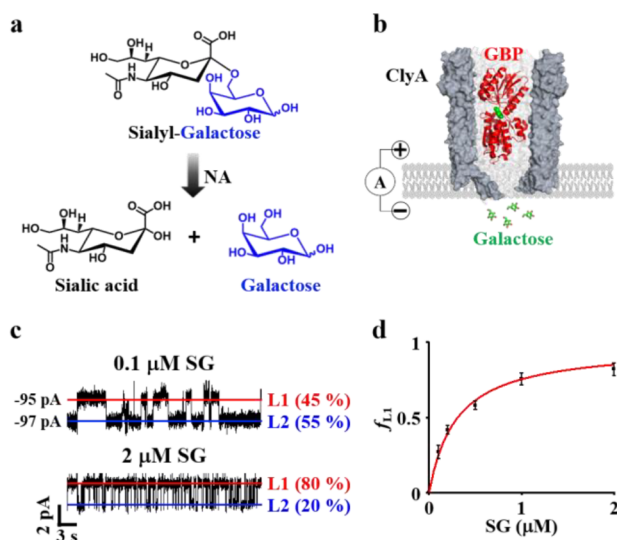


Figure 2. Dependency of the concentrations of the SG substrate on the IAV NA enzymatic activity. (a) Illustration of substrate cleavage by IAV NA. Sialyl-galactose (SG) is a natural substrate of IAV NA. NA cleaves SG, producing sialic acid and galactose. (b) Illustration of the detection mechanism of galactose by the ClyA nanopore using the conformational change of the trapped GBP. (c) Current traces were monitored at increasing concentrations of the SG substrate. Indicated concentrations of SG were preincubated with NA (5 mU mL^{-1}) for 1 h before addition to the GBP-trapped ClyA nanopore. (d) Fractional times of L1 (f_{L1}) versus concentrations of the SG substrate fitted to a Hill function with the coefficient set to 1. Error bars represent standard deviation ($N = 3$).

constriction of ClyA (3.3 nm) and bind to the trapped GBP added to the *cis* chamber, while large molecules such as NA ($4.6 \text{ nm} \times 5.0 \text{ nm} \times 5.6 \text{ nm}$) cannot enter the narrow *trans* side of the nanopore. The concentration of SG was increased from 0.1 to $50 \mu\text{M}$ in the presence of NA (5 mU mL^{-1}). As the concentration of SG increased, the relative event duration of L1 was demonstrated to increase from 45% to 80% (from 0.27 to 0.82 in f_{L1}) (Figure 2c). Accordingly, the duration of L1 events was observed to be significantly increased until the achieved saturation at the SG substrate concentration of $50 \mu\text{M}$. As shown in Figure 2d, the fractional times of L1 (f_{L1}) according to the SG concentration were fitted to a Hill function with the coefficient set to 1. The K_d^{app} value ($0.3 \pm 0.03 \mu\text{M}$) determined by the SG-cleaved galactose was shown to be similar to those measured using purified galactose ($0.23 \pm 0.02 \mu\text{M}$). These data indicated that this GBP-trapped ClyA nanopore could monitor the concentration of galactose produced during the SG cleavage process by the NA enzyme.

Next, we performed a nanopore experiment for real-time monitoring of the enzymatic activity of NA using the ClyA nanopore. With increasing the enzymatic reaction time of NA at the applied voltage of -90 mV , the relative event duration of L1 was observed to be substantially increased to 80% in 30 min, indicating that the prolonged activity of NA led to the increased concentration of galactose (Figure 3a). In the absence of the NA enzyme, the SG substrate or sialic acid did not induce any interference on the current blockades of the GBP-trapped ClyA nanopore (Figure 3b). Taken together, these results showed that the GBP-trapped ClyA nanopore could be utilized for the real-time detection of the enzymatic activity of NA. This nanopore sensor exhibited rapid detection of the NA of influenza virus in $\sim 10 \text{ min}$ after sample loading, a

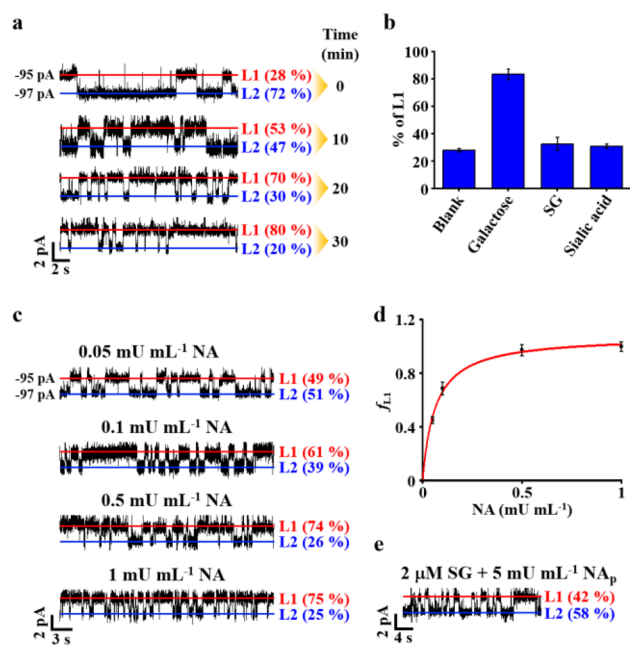


Figure 3. Real-time detection and dependency of enzymatic concentrations in the IAV NA enzymatic activity. (a) Real-time analysis of the enzymatic activity of NA. SG substrate ($2 \mu\text{M}$) and NA (35 mU mL^{-1}) were added to the *trans* compartment of the GBP-trapped ClyA nanopore. Electric current traces were measured in real-time for 30 min, and then, the relative event durations of L1 were analyzed for each 10 min nanopore data. (b) Comparison of the relative event durations of L1 obtained from galactose, SG, and sialic acid. Each compound was independently added to the *trans* compartment of the GBP-trapped ClyA nanopore without NA to analyze background signals. (c) Current traces obtained at increasing concentrations of the NA enzyme. (d) Fractional times of L1 (f_{L1}) versus the concentrations of the NA enzyme fitted to a Hill function with the coefficient set to 1. Error bars represent standard deviation ($N = 3$). (e) Measurement using a negative control, namely, the NA (NA_p) enzyme from *Streptococcus pneumoniae*.

significant advantage over other time-consuming diagnostic methods.

To obtain a calibration curve for the activity of NA, we performed nanopore experiments at various concentrations of NA (0.05 to 5 mU mL^{-1}) in the presence of $2 \mu\text{M}$ SG. We chose $2 \mu\text{M}$ SG after testing various substrate concentrations ranging from 0.1 to $50 \mu\text{M}$ because a nearly full saturation of NA enzymatic activity (f_{L1}) was achieved at $2 \mu\text{M}$ (Figure 2d). In addition, the detection condition was determined based on previous reports on glucose detection by ClyA nanopores.¹⁶ As the concentration of NA increased, the relative event duration of L1 was observed to increase from $\sim 49\%$ to $\sim 75\%$ in each independent experiment ($N = 3$) (Figure 3c). The dependence of f_{L1} to the concentration of NA was fitted well to a Hill function (Figure 3d). We found that the galactose-bound fraction (the closed conformation of GBP) was saturated at the concentration of 1 mU mL^{-1} of NA. These results indicated that the GBP-trapped ClyA nanopore could allow the quantification of NA, which is applicable for IAV diagnostics. Moreover, the limit of detection of NA (LOD^{NA}) using the GBP-trapped ClyA nanopore was shown to be 0.17 ng mL^{-1} , indicating that this nanopore sensor has 40–80-fold higher sensitivity than conventional methods, such as electrochemical assay (14.8 ng mL^{-1})³⁷ and ELISA immunocapture assay (7 ng mL^{-1}) (Table S1).³⁸ On the basis of these data, we assumed

that the number of viral particles could be quantitatively estimated using the nanopore sensor. Approximately 50 copies of NA are known to exist as tetramers on the surface of IAV, and thus, there are 200 individual NA units capable of cleaving sialic acids.⁵ On the basis of this, the concentration of NA for LOD^{NA} (0.17 ng mL⁻¹) could be converted to approximately 8.4×10^9 viral particles.

As a negative control for our nanopore experiments, we monitored the enzymatic activity of the bacterial NA from *Streptococcus pneumoniae* (NA_p) using the GBP-trapped ClyA nanopore. We observed that the relative event duration of L1 was not significantly changed compared with that for SG only (Figure 3e). In contrast to IAV NA, NA_p is known to cleave SG at a negligible rate as it has been reported that it cannot recognize the α -2,6 glycosidic bond of SG.³⁶ Therefore, this GBP-trapped ClyA nanopore sensor could be useful for monitoring viral or bacterial NA enabled to cleave a SG substrate with α -2,6 linkage. For monitoring the activity of other viral or bacterial NA, the SG substrate could be easily substituted with any substrate to improve specificity.

The NA inhibitors, including oseltamivir (Tamiflu) and zanamivir (Relenza) belong to a representative class of FDA-approved antiviral drugs against IAV. The determination of the crystal structure and catalytic site of NA was the crucial step that led to the development of zanamivir and oseltamivir. These inhibitors were developed through modification of the sialic acid substrate or structural analogs, fitting into the active site framework of NA. Briefly, NA inhibitors are known to effectively interfere with the release of progeny IAV from infected host cells. However, sequential mutations in or around the active site of NA have been shown to increase drug resistance against NA inhibitors.^{39,40} Fortunately, the 2009 IAV pandemic was an oseltamivir-sensitive IAV strain. However, the rapid emergence and transmission of oseltamivir-resistant IAV viral strains are threatening, and therefore, a drug susceptibility test of diverse viral strains, as well as the development of novel antiviral drugs, are clinically important.⁴¹ In case a viral strain is not resistant to an antiviral drug, the action of the viral NA would be blocked, and thus, no released galactose would be detected. To test the potential application of this nanopore sensor to a drug susceptibility test or drug screening, we investigated the inhibition effect of the activity of NA using the GBP-trapped ClyA nanopore with antiviral inhibitors, such as oseltamivir carboxylate (OC), zanamivir (ZN), braziliin (BZ), and epicatechin (EC) (Figure 4a). In previous studies, it was shown that OC and ZN are potent, specific, and well-known inhibitors of IAV NA with IC₅₀ values of 0.45 and 0.95 nM, respectively, whereas BZ and EC with IC₅₀ values of 0.2 and >100 μ M, respectively, were reported to exhibit reduced inhibition effects relative to that of OC.^{42–44} Vanillic acid (VA) was used as a negative control. Following incubation of 2 μ M SG and 5 mU mL⁻¹ NA with 1 μ M OC, ZN, BZ, EC, or VA at 37 °C for 1 h, we measured the relative event durations of L1 using the GBP-trapped ClyA nanopore. Although the relative event durations of L1 were shown to be increased to 75% in the absence of NA inhibitors, we observed a significant decrease of these values in the presence of inhibitors, except for VA (Figure 4b). The relative event durations of L1 in the presence of OC and ZN decreased to 38% and 40%, respectively, indicating that both OC and ZN inhibit NA activity of SG cleavage and galactose release. Similarly, the relative event durations of L1 for the treatments with BZ and EC were decreased to 47% and 55%, respectively,

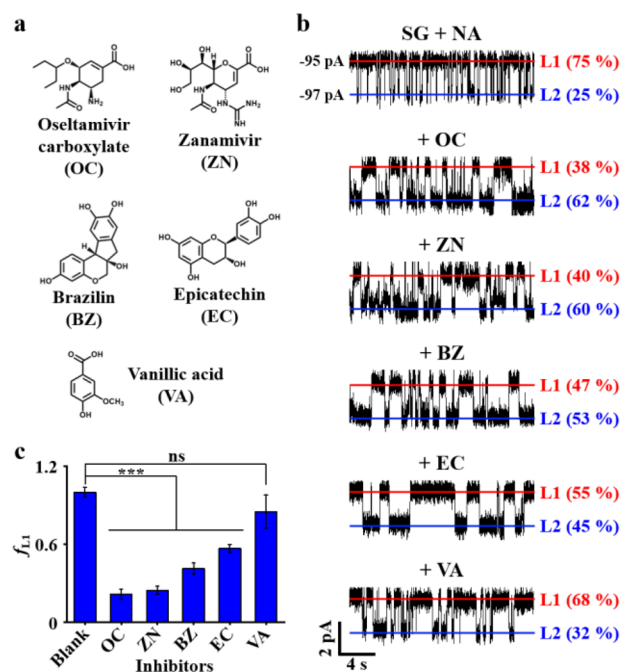


Figure 4. Nanopore-based measurement of the inhibition of IAV NA by antiviral drugs. (a) Small-molecule inhibitors of IAV NA. (b) Current traces obtained from the enzymatic reaction of NA with each of the inhibitors. SG substrate (2 μ M) and NA (5 mU mL⁻¹) were preincubated with OC, ZN, BZ, EC, or VA. Each mixture was independently treated to the *trans* compartment of the GBP-trapped ClyA nanopore. (c) Comparison of fractional times of L1 (f_{L1}) obtained from the enzymatic reaction of NA with each of the inhibitors. The f_{L1} values of each inhibitor were analyzed using a two-tailed Student's *t*-test. Error bars represent standard deviation. ****p* < 0.001; ns = no significance.

with their inhibitory effects being less than those of OC and ZN. Comparing the f_{L1} for these inhibitory effects (Figure 4c), we found that the order of the inhibition of NA (OC \cong ZN > BZ > EC) was consistent with the previously reported IC₅₀ values.^{42–44} Taken together, we suggest that a GBP-trapped ClyA nanopore could be used to rapidly monitor the inhibitory effect of antiviral drugs on viral NA activities, which has important implications in drug susceptibility testing and screening of novel small-molecule antagonists.

In summary, we showed the application of a ClyA protein nanopore to probe the enzymatic activity of NA by sensing the galactose cleaved from SG substrates. Owing to the robust advantages of its single-molecule detection, the ClyA nanopore sensor showed remarkable high sensitivity for the detection of NA; the resultant LOD^{NA} was estimated to be 0.17 ng mL⁻¹, which is 40–80-fold lower than those previously reported.^{37,38,45} Furthermore, we monitored the inhibitory effect of antiviral drugs on the activity of NA in real time using the GBP-trapped ClyA nanopore. Our findings suggested that the nanopore sensor could be used to rapidly test the drug susceptibility, compared with current genotypic and phenotypic methods that take time (several hours) and resources (trained personnel and instruments). The protein nanopore sensor could also be utilized as a novel approach for the sensitive and label-free screening of antiviral drugs against NA. Taken together, our results suggest that a nanopore-based sensor of the activity of NA could serve as a rapid and

ultrasensitive platform for the early point-of-care diagnosis and drug screening of influenza.

■ ASSOCIATED CONTENT

Supporting Information

The Supporting Information is available free of charge at <https://pubs.acs.org/doi/10.1021/acs.analchem.0c03399>.

Table S1, experimental section, and references (PDF)

■ AUTHOR INFORMATION

Corresponding Author

Seung-Wook Chi – Disease Target Structure Research Center, Division of Biomedical Research, KRIBB, Daejeon 34141, Republic of Korea; Department of Proteome Structural Biology, KRIBB School of Bioscience, University of Science and Technology, Daejeon 34113, Republic of Korea; orcid.org/0000-0001-9381-3251; Email: swchi@kribb.re.kr

Authors

Dong-Kyu Kwak – Disease Target Structure Research Center, Division of Biomedical Research, KRIBB, Daejeon 34141, Republic of Korea; Department of Proteome Structural Biology, KRIBB School of Bioscience, University of Science and Technology, Daejeon 34113, Republic of Korea

Jin-Sik Kim – Disease Target Structure Research Center, Division of Biomedical Research, KRIBB, Daejeon 34141, Republic of Korea

Mi-Kyung Lee – Disease Target Structure Research Center, Division of Biomedical Research, KRIBB, Daejeon 34141, Republic of Korea; orcid.org/0000-0003-4771-7861

Kyoung-Seok Ryu – Protein Structure Research Group, Korea Basic Science Institute, Ochang-eup, Cheongju-si, Chungcheongbuk-do 28119, Republic of Korea; orcid.org/0000-0002-8422-6669

Complete contact information is available at: <https://pubs.acs.org/doi/10.1021/acs.analchem.0c03399>

Author Contributions

[†]D.-K. Kwak and J.-S. Kim contributed equally.

Notes

The authors declare no competing financial interest.

■ ACKNOWLEDGMENTS

The authors would like to thank Prof. Giovanni Maglia at the University of Groningen, The Netherlands, for kindly providing a recombinant plasmid encoding the type I ClyA-AS gene and Dr. Si-Eun Sung, KRIBB, for helping with GBP protein purification. This work was supported by National Research Foundation grants funded by the Korean government (MSIT) (NRF-2017R1E1A1A01074403, NRF-2019M3E5D4069903, and NRF-2019M3A9C4076156 to S.-W.C.) and by the KRIBB Research Initiative Program (to S.-W.C.).

■ REFERENCES

(1) Iuliano, A. D.; Roguski, K. M.; Chang, H. H.; Muscatello, D. J.; Palekar, R.; Tempia, S.; Cohen, C.; Gran, J. M.; Schanzer, D.; Cowling, B. J.; Wu, P.; Kyncl, J.; Ang, L. W.; Park, M.; Redlberger-Fritz, M.; Yu, H.; Espenhain, L.; Krishnan, A.; Emukule, G.; van Asten, L.; Pereira da Silva, S.; Aungkulanon, S.; Buchholz, U.; Widdowson, M.-A.; Bresee, J. S.; Azziz-Baumgartner, E.; Cheng, P.-Y.; Dawood, F.; Foppa, I.; Olsen, S.; Haber, M.; Jeffers, C.; MacIntyre, C.

R.; Newall, A. T.; Wood, J. G.; Kundi, M.; Popow-Kraupp, T.; Ahmed, M.; Rahman, M.; Marinho, F.; Sotomayor Proschle, C. V.; Vergara Mallegas, N.; Luzhao, F.; Sa, L.; Barbosa-Ramirez, J.; Sanchez, D. M.; Gomez, L. A.; Vargas, X. B.; Acosta Herrera, A.; Llanes, M. J.; Fischer, T. K.; Krause, T. G.; Mølbak, K.; Nielsen, J.; Trebbien, R.; Bruno, A.; Ojeda, J.; Ramos, H.; an der Heiden, M.; del Carmen Castillo Signor, L.; Serrano, C. E.; Bhardwaj, R.; Chadha, M.; Narayan, V.; Kosen, S.; Bromberg, M.; Glatman-Freedman, A.; Kaufman, Z.; Arima, Y.; Oishi, K.; Chaves, S.; Nyawanda, B.; Al-Jarallah, R. A.; Kuri-Morales, P. A.; Matus, C. R.; Corona, M. E. J.; Burmaa, A.; Darmaa, O.; Obtel, M.; Cherkaoui, I.; van den Wijngaard, C. C.; van der Hoek, W.; Baker, M.; Bandaranayake, D.; Bissielo, A.; Huang, S.; Lopez, L.; Newbern, C.; Flem, E.; Grøneng, G. M.; Hauge, S.; de Cosio, F. G.; de Molto, Y.; Castillo, L. M.; Cabello, M. A.; von Horoch, M.; Medina Osis, J.; Machado, A.; Nunes, B.; Rodrigues, A. P.; Rodrigues, E.; Calomfirescu, C.; Lupulescu, E.; Popescu, R.; Popovici, O.; Bogdanovic, D.; Kostic, M.; Lazarevic, K.; Milosevic, Z.; Todorovic, B.; Chen, M.; Cutter, J.; Lee, V.; Lin, R.; Ma, S.; Cohen, A. L.; Treurnicht, F.; Kim, W. J.; Delgado-Sanz, C.; de mateo Ontanon, S.; Larrauri, A.; Leon, I. L.; Vallejo, F.; Born, R.; Junker, C.; Koch, D.; Chuang, J.-H.; Huang, W.-T.; Kuo, H.-W.; Tsai, Y.-C.; Bundhamcharoen, K.; Chittaganpitch, M.; Green, H. K.; Pebody, R.; Goni, N.; Chiparelli, H.; Brammer, L.; Mustaqim, D. *Lancet* **2018**, 391 (10127), 1285–1300.

(2) Sovinova, O.; Tumova, B.; Pouska, F.; Nemeč, J. *Acta Virol.* **1958**, 2 (1), 52–61.

(3) Geraci, J. R.; St Aubin, D. J.; Barker, I. K.; Webster, R. G.; Hinshaw, V. S.; Bean, W. J.; Ruhnke, H. L.; Prescott, J. H.; Early, G.; Baker, A. S.; Madoff, S.; Schooley, R. T. *Science* **1982**, 215 (4536), 1129–31.

(4) Shope, R. E. *J. Exp. Med.* **1931**, 54 (3), 349–59.

(5) McAuley, J. L.; Gilbertson, B. P.; Trifkovic, S.; Brown, L. E.; McKimm-Breschkin, J. L. *Front. Microbiol.* **2019**, 10, 39.

(6) Wu, X.; Wu, X.; Sun, Q.; Zhang, C.; Yang, S.; Li, L.; Jia, Z. *Theranostics* **2017**, 7 (4), 826–845.

(7) Grienke, U.; Schmidtke, M.; von Grafenstein, S.; Kirchmair, J.; Liedl, K. R.; Rollinger, J. M. *Nat. Prod. Rep.* **2012**, 29 (1), 11–36.

(8) Corfield, T. *Glycobiology* **1992**, 2 (6), 509–21.

(9) von Itzstein, M. *Nat. Rev. Drug Discovery* **2007**, 6 (12), 967–74.

(10) Moscona, A. *N. Engl. J. Med.* **2005**, 353 (13), 1363–73.

(11) Palese, P.; Tobita, K.; Ueda, M.; Compans, R. W. *Virology* **1974**, 61 (2), 397–410.

(12) Dziabowska, K.; Czaczyk, E.; Nidzworski, D. *Biosensors* **2018**, 8 (4), 94.

(13) Tobita, K.; Sugiura, A.; Enomoto, C.; Furuyama, M. *Med. Microbiol. Immunol.* **1975**, 162 (1), 9–14.

(14) Novak-Weekley, S. M.; Marlowe, E. M.; Poulter, M.; Dwyer, D.; Speers, D.; Rawlinson, W.; Baleriola, C.; Robinson, C. C. *J. Clin. Microbiol.* **2012**, 50 (5), 1704–10.

(15) Trombetta, V. K.; Chan, Y. L.; Bankowski, M. J. *Hawaii J. Med. Public Health* **2018**, 77 (9), 226–230.

(16) Galenkamp, N. S.; Soskine, M.; Hermans, J.; Wloka, C.; Maglia, G. *Nat. Commun.* **2018**, 9 (1), 4085.

(17) Bayley, H. *Clin. Chem.* **2015**, 61 (1), 25–31.

(18) Kasianowicz, J. J.; Brandin, E.; Branton, D.; Deamer, D. W. *Proc. Natl. Acad. Sci. U. S. A.* **1996**, 93 (24), 13770–3.

(19) Majd, S.; Yusko, E. C.; Billeh, Y. N.; Macrae, M. X.; Yang, J.; Mayer, M. *Curr. Opin. Biotechnol.* **2010**, 21 (4), 439–76.

(20) Shi, W.; Friedman, A. K.; Baker, L. A. *Anal. Chem.* **2017**, 89 (1), 157–188.

(21) Cao, C.; Long, Y. T. *Acc. Chem. Res.* **2018**, 51 (2), 331–341.

(22) Kwak, D. K.; Chae, H.; Lee, M. K.; Ha, J. H.; Goyal, G.; Kim, M. J.; Kim, K. B.; Chi, S. W. *Angew. Chem., Int. Ed.* **2016**, 55 (19), 5713–7.

(23) Chae, H.; Kwak, D. K.; Lee, M. K.; Chi, S. W.; Kim, K. B. *Nanoscale* **2018**, 10 (36), 17227–17235.

(24) Oh, S.; Lee, M. K.; Chi, S. W. *ACS Sens* **2019**, 4 (11), 2849–2853.

- (25) Soskine, M.; Biesemans, A.; De Maeyer, M.; Maglia, G. *J. Am. Chem. Soc.* **2013**, *135* (36), 13456–63.
- (26) Zernia, S.; van der Heide, N. J.; Galenkamp, N. S.; Gouridis, G.; Maglia, G. *ACS Nano* **2020**, *14*, 2296.
- (27) Wloka, C.; Van Meervelt, V.; van Gelder, D.; Danda, N.; Jager, N.; Williams, C. P.; Maglia, G. *ACS Nano* **2017**, *11* (5), 4387–4394.
- (28) Biesemans, A.; Soskine, M.; Maglia, G. *Nano Lett.* **2015**, *15* (9), 6076–6081.
- (29) Zukin, R. S.; Strange, P. G.; Heavey, R.; Koshland, D. E. *Biochemistry* **1977**, *16* (3), 381–6.
- (30) Borrok, M. J.; Kiessling, L. L.; Forest, K. T. *Protein Sci.* **2007**, *16* (6), 1032–41.
- (31) Unione, L.; Ortega, G.; Mallagaray, A.; Corzana, F.; Perez-Castells, J.; Canales, A.; Jimenez-Barbero, J.; Millet, O. *ACS Chem. Biol.* **2016**, *11* (8), 2149–57.
- (32) Soskine, M.; Biesemans, A.; Moeyaert, B.; Cheley, S.; Bayley, H.; Maglia, G. *Nano Lett.* **2012**, *12* (9), 4895–900.
- (33) Li, X.; Lee, K. H.; Shorkey, S.; Chen, J.; Chen, M. *ACS Nano* **2020**, *14* (2), 1727–1737.
- (34) Sakaguchi-Mikami, A.; Taneoka, A.; Yamoto, R.; Ferri, S.; Sode, K. *Biotechnol. Lett.* **2008**, *30* (8), 1453–60.
- (35) Armbruster, D. A.; Pry, T. *Clin. Biochem. Rev.* **2008**, *29* (Suppl1), S49–52.
- (36) Cui, X.; Das, A.; Dhawane, A. N.; Sweeney, J.; Zhang, X.; Chivukula, V.; Iyer, S. S. *Chem. Sci.* **2017**, *8* (5), 3628–3634.
- (37) Wahyuni, W. T.; Ivandini, T. A.; Saepudin, E.; Einaga, Y. *Anal. Biochem.* **2016**, *497*, 68–75.
- (38) Gerentes, L.; Kessler, N.; Aymard, M. J. *Virol. Methods* **1998**, *73* (2), 185–95.
- (39) Collins, P. J.; Haire, L. F.; Lin, Y. P.; Liu, J.; Russell, R. J.; Walker, P. A.; Martin, S. R.; Daniels, R. S.; Gregory, V.; Skehel, J. J.; Gamblin, S. J.; Hay, A. J. *Vaccine* **2009**, *27* (45), 6317–23.
- (40) McKimm-Breschkin, J. L. *Influenza Other Respir. Viruses* **2013**, *7* (Suppl 1), 25–36.
- (41) Abed, Y.; Baz, M.; Boivin, G. *Antivir. Ther.* **2006**, *11* (8), 971–6.
- (42) Jeong, H. J.; Kim, Y. M.; Kim, J. H.; Kim, J. Y.; Park, J. Y.; Park, S. J.; Ryu, Y. B.; Lee, W. S. *Biol. Pharm. Bull.* **2012**, *35* (5), 786–90.
- (43) Liu, A. L.; Shu, S. H.; Qin, H. L.; Lee, S. M.; Wang, Y. T.; Du, G. H. *Planta Med.* **2009**, *75* (4), 337–9.
- (44) Liu, A. L.; Wang, H. D.; Lee, S. M.; Wang, Y. T.; Du, G. H. *Bioorg. Med. Chem.* **2008**, *16* (15), 7141–7.
- (45) Yang, W.; Liu, X.; Peng, X.; Li, P.; Wang, T.; Tai, G.; James Li, X.; Zhou, Y. *Carbohydr. Res.* **2012**, *359*, 92–6.